IEEJ Journal of Industry Applications
Vol.8 No.4 pp.600–607 DOI: 10.1541/ieejjia.8.600

Paper

Development of Three-Phase Wireless Power Transfer System with Reduced Radiation Noise

Keisuke Kusaka* Member, Keita Furukawa* Student Member
Jun-ichi Itoh*a) Senior Member

(Manuscript received June 12, 2018, revised April 10, 2019)

A three-phase wireless power transfer (WPT) system, which has six primary coils and six secondary coils is proposed in this paper. The three-phase WPT system reduces the radiation noise by canceling the noise using pairs of coils placed opposite to each other. However, a magnetic interference among the multiple coils decreases the transmission efficiency due to a circulating current among the primary coils, and the secondary coils in WPT systems with multiple coils. The proposed three-phase WPT system cancels out the effect due to the interference among the six coils on each side. First, the WPT system with the 12 coils is proposed. Then, a canceling condition of the magnetic interference among the coils is mathematically introduced from the voltage equation on the coils. Finally, the proposed WPT system is experimentally demonstrated with the 3-kW prototype. The experimental result shows that the radiation noise at the fundamental frequency is suppressed from 12.2 dBμA to 2.1 dBμA.

Keywords: inductive power transfer, wireless power transfer, three-phase, solenoid coil

1. Introduction

In this decade, wireless power transfer (WPT) systems for electrical vehicles (EVs) are actively studied [(1)–(11)] because WPT systems will improve the usability of EVs. Standardization of the WPT system for EVs is ongoing for interoperability [(12)(13)]. The international standard, which will be published by IEC/ISO will classify the WPT system into five classes by the maximum input power. The maximum input power of WPT1 is 3.7 kW or less. The maximum input power of WPT 2 is larger than 3.7 kW, and 7.7 kW or less. The maximum input power of WPT3 is larger than 7.7 kW, and 11 kW or less. The maximum input power of WPT4 is larger than 11 kW, and 22 kW or less. The maximum input power of WPT5 is larger than 22 kW [(12)(13)]. Currently, the standardization of WPT1 and WPT2 is in progress. However, the standardization of high-power WPT systems such as WPT4 or 5 has not been discussed well despite strong demand for higher power WPT system for heavy-duty vehicles. One of the difficulties of the high-power WPT system is heat generation of transmission coils because copper loss and iron loss increase [(14)]. The second is radiation noise. The radiation noise from the WPT system must be suppressed to satisfy the regulations, which are published by CISPR or legislated in each country or region. However, the satisfaction of regulations becomes further difficult because the radiation noise caused by the loop coil is, in principle, increased in proportion to the current on the loop coil [(15)].

As a previous study, a radiation noise reduction method by a duplicated 44-kW WPT system for heavy-duty vehicles has been proposed [(14)(16)(17)]. In (16), the radiation noise is reduced by duplicated transmission coils. The two transmission coils with differential current are placed to reduce the leakage radiation noise. However, the duplicated WPT system limits freedom of coil positions because the magnetic interference is caused by the magnetic coupling between the duplicated coils [(16)]. The magnetic interference decreases power factor of fundamental wave regarding an inverter output.

Meanwhile, three-phase WPT systems have been proposed to increase the output power of the WPT system [(18)–(21)]. The three-phase WPT systems allow the reduction of the current on each transmission coil. Thus the three-phase WPT is has a possibility to reduce the copper loss and the iron loss. However, a magnetic interference among the additional coils on each side occurs in the conventional three-phase WPT system. The magnetic interference does not contribute power transmission between the primary side and the secondary side. The magnetic interference causes an interfering induced voltage on each coils. So, it causes the circulating currents among the primary coils and the secondary coils.

This paper proposes a three-phase WPT system with 12 solenoid coils. The six pairs of coils placed opposite to each other contributes reducing the current on the winding without a byproduct such as a magnetic interference. A contribution of this paper is offering the new transmission coil structure, which reduces the radiation noise with a small effect on efficiency. In the proposed system, the countercurrent in the opposite coils cancel out the radiation noise. Moreover, the primary coils and the secondary coils are placed at an angle of 60 degrees to each other. Consequently, the induced voltage caused by magnetic interference among the 12 coils are canceled out. First, a system configuration of the proposed WPT system is described. Next, a design procedure of the proposed three-phase WPT system with a star-star winding

a) Correspondence to: Jun-ichi Itoh. E-mail: itoh@vos.nagaokaut.ac.jp
* Nagaoka University of Technology
1603-1, Kamitomioka, Nagaoka, Niigata 940-2188, Japan

© 2019 The Institute of Electrical Engineers of Japan.

and a delta-delta winding is explained. Then, the canceling method of the magnetic interference among the multiple coils is mathematically introduced. Finally, the proposed WPT system with star-star winding is tested with a 3-kW prototype. Then, the radiation noise is assessed and compared between the conventional three-phase WPT system and the proposed three-phase WPT system with 12 coils.

2. Three-phase WPT System with 12 Coils

In this chapter, the three-phase WPT system is proposed. The proposed WPT system achieves radiation noise reduction using 12 coils without magnetic interference among multiple coils.

2.1 System Configuration Figure 1 shows the proposed three-phase WPT system with 12 coils. The three-phase coils can be connected with not only star-star winding but also delta-delta, star-delta, and delta-star windings. In this paper, only star-star and delta-delta windings are explained due to the page limitation. In the proposed system, the power is inductively transmitted through the six primary coils and the six secondary coils. Each phase has two coils connected in series. These pairs of coils connected in series cancel out the radiation noise because the magnetic flux direction is opposite owing to the countercurrent flowing on the coils [14].

Besides, the three-phase inverter on the primary side and the three-phase rectifier in the secondary side are used. The primary inverter output square-wave voltage in each phase. The phase differences of each phase are 120 degrees. Furthermore, resonant capacitors are connected to the output of the primary inverter and the input of the rectifier in series. The series-series compensation technique [22] is applied to the proposed system in order to cancel out the leakage inductance due to the weak magnetic coupling. Using three-phase WPT and the series-series compensation technique, copper loss of the windings can be reduced because the current is shunted into six coils. Therefore, the proposed WPT system is effective to improve the heat dissipation of the transmission coils.

Figure 2 illustrates the placement of the transmission coils. In the proposed WPT system, six solenoid coils are used in each of the primary side and the secondary side. Figure 3 shows the mechanism of the reduction in radiation noise using the pairs of coils. Two transmission coils connected in series (e.g., L_{uv1A} and L_{uv1B}) are differentially connected and are placed in an opposite place. These opposite coils cancel out radiation noise at a measurement point, which is typically 10 m from the WPT system [23]. Other pairs of coils are placed in an angle of 120 degrees to the coils on phase-u each other. As a drawback of the reduction in radiation noise using opposite coils, magnetic interference occur among the six coils on each the primary side and the secondary side. The position relationship and figure of the coils have to be adjusted in order to cancel out the magnetic interference. The design method of the coils will be explained in section 2.3.

2.2 Mathematical Model of Three-phase Coils Equations (1) and (2) represents the induced voltage of 12 coils on the star-star winding system and the delta-delta winding system, respectively where L_{1Ys} is the self-inductance of the primary coil on the star-star winding, $L_{1\Delta s}$ is the self-inductance of the primary coil on the delta-delta winding.

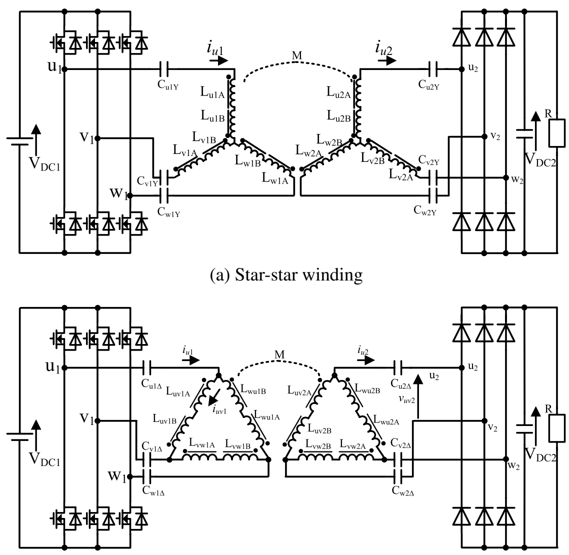

(a) Star-star winding

(b) Delta-delta winding

Fig. 1. Proposed three-phase IPT system with 12 coils

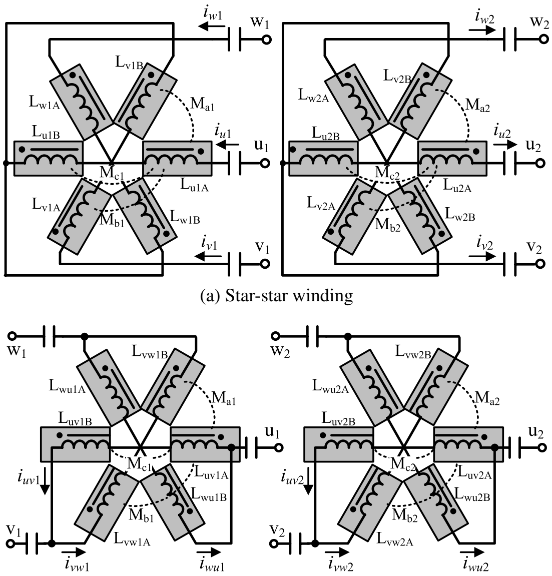

(a) Star-star winding

(b) Delta-delta winding

Fig. 2. Placement and connection of coils

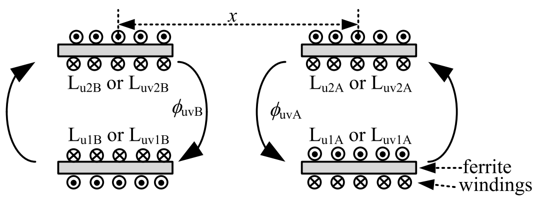

Fig. 3. Mechanism of reduction in radiation noise using solenoid coils

The symbol M represents the mutual inductances between the primary coils and the secondary coils, which contributes to the power transmission, e.g., the mutual inductance between L_{u1A} and L_{u2A}. The suffix "1" indicates coils on the primary side, and "2" means coils on the secondary side. The symbol M_a represents the mutual inductance between the adjacent coils, e.g., the mutual inductance between L_{u1A} and L_{v1B}. The mutual inductance M_b represents the mutual

$$\begin{pmatrix} v_{u1A} \\ v_{u1B} \\ v_{v1A} \\ v_{v1B} \\ v_{w1A} \\ v_{w1B} \\ v_{u2A} \\ v_{u2B} \\ v_{v2A} \\ v_{v2B} \\ v_{w2A} \\ v_{w2B} \end{pmatrix} = \begin{pmatrix} L_{1Ys} & M_{c1} & M_{b1} & M_{a1} & M_{b1} & M_{a1} & M & 0 & 0 & 0 & 0 & 0 \\ M_{c1} & L_{1Ys} & M_{a1} & M_{b1} & M_{a1} & M_{b1} & 0 & M & 0 & 0 & 0 & 0 \\ M_{b1} & M_{a1} & L_{1Ys} & M_{c1} & M_{b1} & M_{a1} & 0 & 0 & M & 0 & 0 & 0 \\ M_{a1} & M_{b1} & M_{c1} & L_{1Ys} & M_{a1} & M_{b1} & 0 & 0 & 0 & M & 0 & 0 \\ M_{b1} & M_{a1} & M_{b1} & M_{a1} & L_{1Ys} & M_{c1} & 0 & 0 & 0 & 0 & M & 0 \\ M_{a1} & M_{b1} & M_{a1} & M_{b1} & M_{c1} & L_{1Ys} & 0 & 0 & 0 & 0 & 0 & M \\ M & 0 & 0 & 0 & 0 & 0 & L_{2Ys} & M_{c2} & M_{b2} & M_{a2} & M_{b2} & M_{a2} \\ 0 & M & 0 & 0 & 0 & 0 & M_{c2} & L_{2Ys} & M_{a2} & M_{b2} & M_{a2} & M_{b2} \\ 0 & 0 & M & 0 & 0 & 0 & M_{b2} & M_{a2} & L_{2Ys} & M_{c2} & M_{b2} & M_{a2} \\ 0 & 0 & 0 & M & 0 & 0 & M_{a2} & M_{b2} & M_{c2} & L_{2Ys} & M_{a2} & M_{b2} \\ 0 & 0 & 0 & 0 & M & 0 & M_{b2} & M_{a2} & M_{b2} & M_{a2} & L_{2Ys} & M_{c2} \\ 0 & 0 & 0 & 0 & 0 & M & M_{a2} & M_{b2} & M_{a2} & M_{b2} & M_{c2} & L_{2Ys} \end{pmatrix} \frac{d}{dt} \begin{pmatrix} i_{u1} \\ -i_{u1} \\ i_{v1} \\ -i_{v1} \\ i_{w1} \\ -i_{w1} \\ i_{u2} \\ -i_{u2} \\ i_{v2} \\ -i_{v2} \\ i_{w2} \\ -i_{w2} \end{pmatrix} \quad \cdots\cdots\cdots (1)$$

$$\begin{pmatrix} v_{uv1A} \\ v_{uv1B} \\ v_{vw1A} \\ v_{vw1B} \\ v_{wu1A} \\ v_{wu1B} \\ v_{uv2A} \\ v_{uv2B} \\ v_{vw2A} \\ v_{vw2B} \\ v_{wu2A} \\ v_{wu2B} \end{pmatrix} = \begin{pmatrix} L_{1\Delta s} & M_{c1} & M_{b1} & M_{a1} & M_{b1} & M_{a1} & M & 0 & 0 & 0 & 0 & 0 \\ M_{c1} & L_{1\Delta s} & M_{a1} & M_{b1} & M_{a1} & M_{b1} & 0 & M & 0 & 0 & 0 & 0 \\ M_{b1} & M_{a1} & L_{1\Delta s} & M_{c1} & M_{b1} & M_{a1} & 0 & 0 & M & 0 & 0 & 0 \\ M_{a1} & M_{b1} & M_{c1} & L_{1\Delta s} & M_{a1} & M_{b1} & 0 & 0 & 0 & M & 0 & 0 \\ M_{b1} & M_{a1} & M_{b1} & M_{a1} & L_{1\Delta s} & M_{c1} & 0 & 0 & 0 & 0 & M & 0 \\ M_{a1} & M_{b1} & M_{a1} & M_{b1} & M_{c1} & L_{1\Delta s} & 0 & 0 & 0 & 0 & 0 & M \\ M & 0 & 0 & 0 & 0 & 0 & L_{2\Delta s} & M_{c2} & M_{b2} & M_{a2} & M_{b2} & M_{a2} \\ 0 & M & 0 & 0 & 0 & 0 & M_{c2} & L_{2\Delta s} & M_{a2} & M_{b2} & M_{a2} & M_{b2} \\ 0 & 0 & M & 0 & 0 & 0 & M_{b2} & M_{a2} & L_{2\Delta s} & M_{c2} & M_{b2} & M_{a2} \\ 0 & 0 & 0 & M & 0 & 0 & M_{a2} & M_{b2} & M_{c2} & L_{2\Delta s} & M_{a2} & M_{b2} \\ 0 & 0 & 0 & 0 & M & 0 & M_{b2} & M_{a2} & M_{b2} & M_{a2} & L_{2\Delta s} & M_{c2} \\ 0 & 0 & 0 & 0 & 0 & M & M_{a2} & M_{b2} & M_{a2} & M_{b2} & M_{c2} & L_{2\Delta s} \end{pmatrix} \frac{d}{dt} \begin{pmatrix} i_{uv1} \\ -i_{uv1} \\ i_{vw1} \\ -i_{vw1} \\ i_{wu1} \\ -i_{wu1} \\ i_{uv2} \\ -i_{uv2} \\ i_{vw2} \\ -i_{vw2} \\ i_{wu2} \\ -i_{wu2} \end{pmatrix} \quad \cdots\cdots\cdots (2)$$

inductance between the coils, which are placed apart from 120 degrees, e.g., the mutual inductance between L_{u1A} and L_{w1A}. The mutual inductance M_c represents the mutual inductance between the opposite coils, e.g., the mutual inductance between L_{u1A} and L_{u1B}. Note that other unwanted mutual inductances, e.g., the mutual inductance between L_{u1A} and L_{u2B} are ignored in Eq. (1).

It is clear from Eq. (1) that the unwanted mutual inductances cause an unwanted induce voltage on each of the transmission coils. This induced voltage decreases efficiency due to a circulating current. The canceling method of these interfering induced voltages will be explained in the next section.

2.3 Cancellation of Magnetic Interference Coupling

In this section, the canceling method of unwanted induced voltage caused by magnetic interference is explained. The cancellation method of the magnetic interference coupling is explained with the star-star winding. However, the cancellation technique can be used for the delta-delta winding.

The induced voltage on L_{u1} is derived from the first column of Eq. (1) as

$$\begin{aligned} v_{u1A} &= L_{1Ys}\frac{di_{u1}}{dt} + M\frac{di_{u2}}{dt} - M_{c1}\frac{di_{u1}}{dt} \\ &\quad - M_{a1}\left(\frac{di_{v1}}{dt} + \frac{di_{w1}}{dt}\right) + M_{b1}\left(\frac{di_{v1}}{dt} + \frac{di_{w1}}{dt}\right). \end{aligned} \quad \cdots\cdots (3)$$

The first term of the right side in Eq. (3) is the induced voltage by the self-inductance, the second term is the mutual inductance caused by the coil on the secondary side. The second term contributes to power transmission. The third to fifth terms are the induced voltage caused by the interference coupling. If the sum of the third to fifth terms of Eq. (3) is zero, the relationship between the primary coil L_{1Ys} and the secondary coil L_{2Ys} is seen as the same as a transmission with one-by-one.

Assuming the three-phase equilibrium, Eq. (3) is transformed as

$$\begin{aligned} v_{u1A} &= L_{1Ys}\frac{di_{u1}}{dt} + M\frac{di_{u2}}{dt} \\ &\quad - \omega I_m \left\{ M_{c1}\cos\omega t + (M_{a1} - M_{b1})\cos\left(\omega t - \frac{2}{3}\pi\right) \right. \\ &\quad \left. (M_{a1} - M_{b1})\cos\left(\omega t - \frac{4}{3}\pi\right) \right\}, \end{aligned} \quad \cdots (4)$$

where I_m is the maximum value of the primary current i_{u1}, which flows in each of the primary coils.

From Eq. (4), it is found that the unwanted induced voltage does not occur when Eq. (5) is satisfied.

$$M_{a1} = M_{b1} + M_{c1} \quad \cdots\cdots (5)$$

Since the self-inductance of the primary coils L_{1Ys} is equal to each other, the canceling condition of the interfering induced voltage is

$$k_{a1} = k_{b1} + k_{c1}. \quad \cdots\cdots (6)$$

Therefore, designing the magnetic coupling among the primary coils according to Eq. (6) cancel out the effect of unwanted coupling on the primary side.

Similarly, the unwanted coupling on the secondary side can be canceled out by designing the magnetic coupling according to Eq. (7).

$$k_{a2} = k_{b2} + k_{c2} \quad \cdots\cdots (7)$$

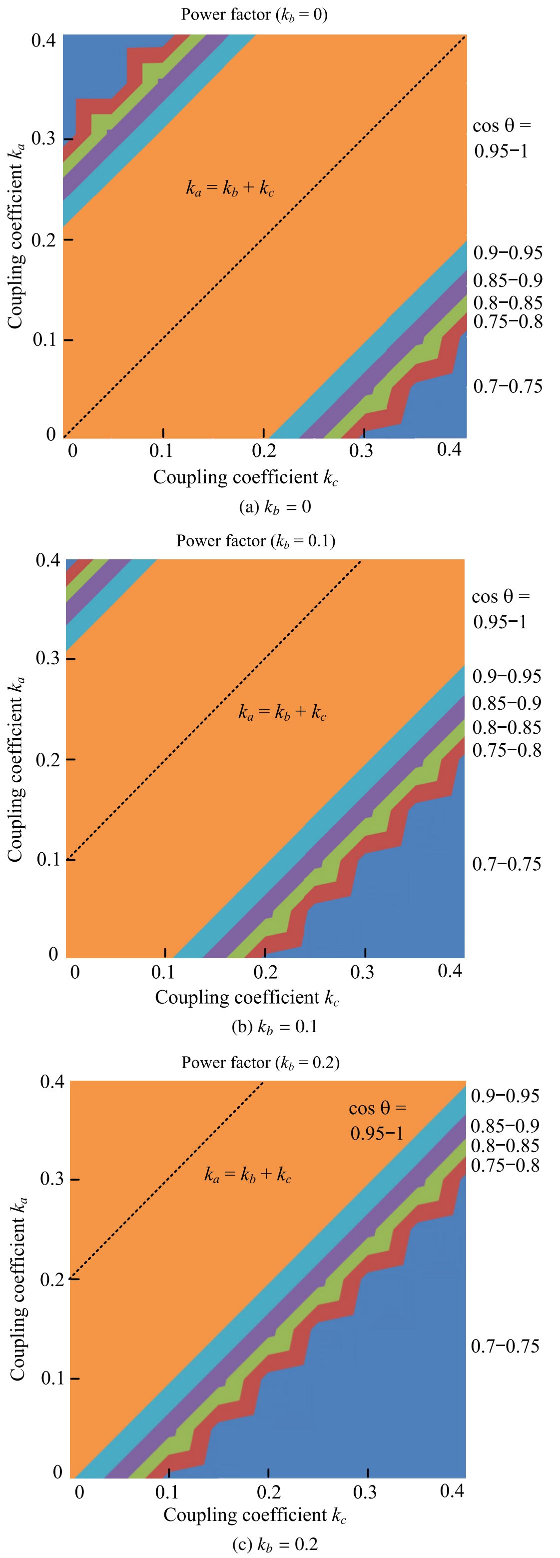

Fig. 4. Effect of magnetic interference coupling on power factor

Figure 4 shows the simulated relationship between the inverter output power factor and the magnetic interference couplings k_a, k_b, and k_c. The dotted line on the graph represents Eq. (6). Figures 4(a), (b), and (c) show the relation when the magnetic interference coupling k_b is zero, 0.1 and 0.2, respectively. When the magnetic interference coupling is small enough to be negligible, the power factor closes to unity. The power factor of the fundamental wave will degrade when the sum of the interference coupling k_b and k_c does not equal to k_a. However, the power factor of fundamental wave remains at high even when the interference couplings increase as long as Eq. (6) is satisfied. In other words, these results show that the magnetic interferences among the transmission coils do not affect the power factor of the fundamental wave when the relation of the interference coupling fits on Eq. (6).

3. Design of Three-phase WPT System

In this chapter, the design method of the proposed three-phase WPT system with the star-tar winding and the delta-delta winding is described. In this design procedure, the induced voltage generated by the magnetic interference among the multiple coils can be ignored with assuming Eqs. (6), (7).

3.1 Star-star Winding The design method of the proposed three-phase WPT system with the star-star winding shown in Fig. 1(a) in this section.

1) Equivalent AC resistance

The equivalent AC resistance is expressed using the rated output voltage V_{DC2}, and rated output power P. The Eq. (8) can be introduced by expanding a derivation of an equivalent AC resistance of a single-phase rectifier to the three-phase rectifier [24]. The equivalent AC resistance for a phase is expressed by

$$R_{eq} = \frac{8}{\pi^2}\frac{(V_{DC2}/2)^2}{P/3} = \frac{6}{\pi^2}\frac{V_{DC2}^2}{P} \quad \cdots\cdots (8)$$

2) Secondary inductance

Maximizing a transmission efficiency, it has been proposed that an impedance of the secondary inductance is equal to the impedance of the equivalent AC resistance [25]. The secondary self-inductance for a certain phase should be (9) by ignoring a winding resistance and assuming the following resonance condition where ω is the transmission angular frequency, k is the coupling coefficient.

$$L_{2Y} = L_{u2} = L_{v2} = L_{w2} = \frac{6}{\pi^2 k\omega}\frac{V_{DC2}^2}{P} \quad \cdots\cdots (9)$$

The secondary inductances have to be half because two transmission coils are connected in each phase in the proposed WPT system. Thus, inductance for a certain coil is $L_{2Ys} = L_{2Y}/2$.

3) Primary inductance

From the voltage ratio between the input DC voltage V_{DC1} and the output DC voltage V_{DC2} under the resonance condition, a primary self-inductance for obtaining the desired rated voltage is expressed by

$$L_{1Y} = L_{u1} = L_{v1} = L_{w1} = L_{2Y}\left(\frac{V_{DC1}}{V_{DC2}}\right)^2 = \frac{6}{\pi^2 k\omega}\frac{V_{DC1}^2}{P}, \quad \cdots\cdots (10)$$

where the primary inverter is operated with a square-wave operation. In the proposed WPT system, the transmission coils are divided and connected in series. The inductances represented by Eq. (10) have to be half. Thus, the inductance of the primary coil is $L_{1Ys} = L_{1Y}\,/\,2$.

4) Resonance capacitors

The resonance capacitors are connected to the output of the primary inverter and the input of the rectifier in series. The resonance capacitors are designed to be resonated with the self-inductance at the transmission angular frequency ω. Thus, the resonant capacitors can be designed as

$$C_{u1Y} = C_{v1Y} = C_{w1Y} = \frac{1}{\omega^2 L_{1Y}}, \quad (11)$$

$$C_{u2Y} = C_{v2Y} = C_{w2Y} = \frac{1}{\omega^2 L_{2Y}}. \quad (12)$$

Note that, the operating frequency is slightly adjusted to achieve a zero-voltage switching of the MOSFETs in the inverter.

3.2 Delta-delta Winding This section describes the design method of the proposed three-phase WPT system with the delta-delta winding shown in Fig. 1(b).

The equivalent resistance for the star connection is as same as the star-star winding.

1) Secondary inductance

The secondary inductance $L_{2\Delta}$ should be equal to the impedance of the equivalent AC resistance. Thus the secondary inductance with a star winding is expressed by

$$L_{2Y} = \frac{R_{eq}}{k\omega} = \frac{6}{\pi^2 k\omega}\frac{V_{DC2}^2}{P} \quad (13)$$

with assuming small winding resistance under the resonance condition.

The secondary inductance expressed by Eq. (13) have to be transformed into the inductance for the delta-delta winding. The secondary inductance is expressed by

$$L_{2\Delta} = L_{uv2} = L_{vw2} = L_{wu2} = 3L_{2Y} = \frac{18}{\pi^2 k\omega}\frac{V_{DC2}^2}{P}. \quad (14)$$

The inductance expressed in Eq. (14) have to be half in the proposed WPT system because the transmission coils are divided and connected in series.

2) Primary inductance

The primary inductance is calculated by Eq. (15) from the voltage ratio between the primary DC voltage and the secondary DC voltage when the primary inverter is operated in square-wave operation mode.

$$L_{1\Delta} = L_{uv1} = L_{vw1} = L_{wu1} = L_{2\Delta}\left(\frac{V_{DC1}}{V_{DC2}}\right)^2 = \frac{18}{\pi^2 k\omega}\frac{V_{DC1}^2}{P} \quad (15)$$

The primary inductances also have to be half.

3) Resonance capacitors

The resonance capacitors are connected in series to the output of the inverter and the input of the rectifier. The resonance capacitors are designed to resonate with the primary and the secondary inductance at the transmission angular frequency ω.

$$C_{u1\Delta} = C_{v1\Delta} = C_{w1\Delta} = \frac{3}{\omega^2 L_{1\Delta}} \quad (16)$$

$$C_{u2\Delta} = C_{v2\Delta} = C_{w2\Delta} = \frac{3}{\omega^2 L_{2\Delta}} \quad (17)$$

4. Experimental Verification

Figure 5 and Table 1 show the prototype and its specifications. In this paper, the proposed WPT system with the star-star winding is experimentally demonstrated. The magnetic interference couplings are $k_a = 0.048$, $k_b = 0.011$, and $k_c = 0.003$. Each transmission coils have ferrite plates of 245 × 215 × 10 mm. The ferrite plates are put into boxes made from acrylic. As windings for the transmission coils, a litz-wire is used.

Figure 6 shows the operation waveforms with the 3-kW prototype. Figure 6(a) shows the inverter output voltage v_{uv1}, output current i_{u1}, rectifier input current i_{u2} and output

(a) Three-phase inverter

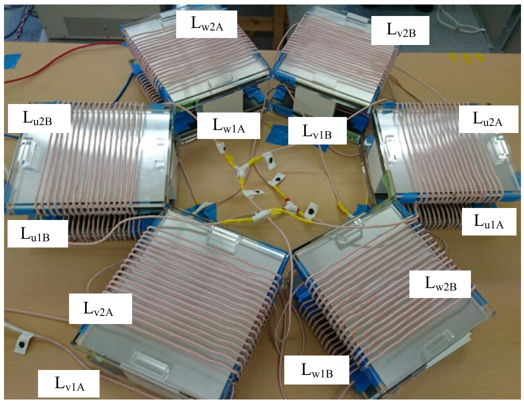

(b) Transmission coils

Fig. 5. 3-kW prototype

Table 1. Specifications of the prototype

Item	Symbol	Value	
Primary DC voltage	V_{DC1}	400	V
Secondary DC voltage	V_{DC2}	400	V
Rated power	P	3	kW
Transmission frequency	f	85.6	kHz
Transmission distance	d	73	mm
Distance between opposite coils	x	655	mm
Coupling coefficient	k	0.26	
Interference coupling	k_a	0.048	
	k_b	0.011	
	k_c	0.003	
Primary inductance	L_{1Ys}	106	uH
Secondary inductance	L_{2Ys}	106	uH
Primary capacitance	$C_{u1Y}, C_{v1Y}, C_{w1Y}$	16.5	nF
Secondary capacitance	$C_{u2Y}, C_{v2Y}, C_{w2Y}$	16.5	nF
MOSFETs	SCT3030AL (ROHM)		
Diodes	VS-20ETF06-M3 (Vishay)		

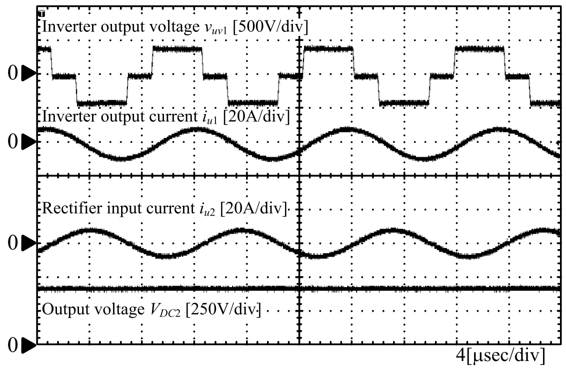

(a) Inverter output voltage, output current, rectifier input current and output voltage

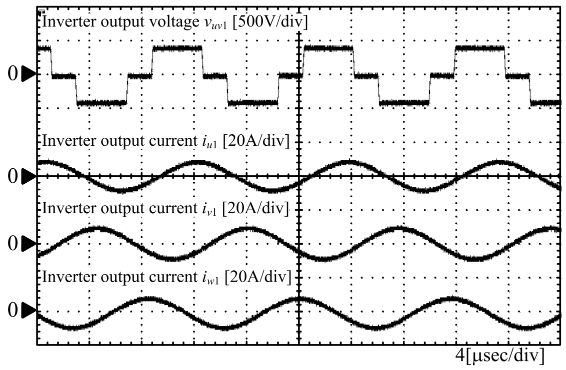

(b) Inverter output voltage and output currents on the primary side

Fig. 6. Operation waveforms

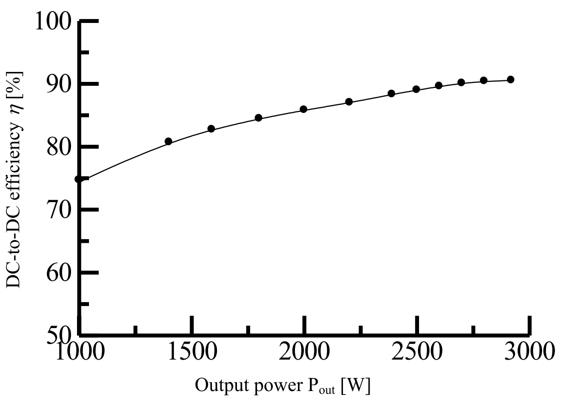

Fig. 7. Efficiency characteristic

voltage V_{DC2}. Note that the line voltage v_{uv1} as the inverter output voltage is observed. Thus, the inverter output current lags 30 degrees with respect to the inverter output linevolage. It means that the power factor of fundamental wave can be corrected when the relationship among the magnetic interference couplings k_a, k_b, and k_c satisfy Eqs. (6), (7). Thus, the effect of the magnetic interference coupling on the power factor is canceled out. Moreover, it is confirmed that power is transmitted from the primary side to the secondary side.

Figure 7 shows the measured efficiency characteristic from the primary DC voltage to the secondary DC voltage. In fact, the efficiency takes into account the power loss in the inverter and the rectifier. The maximum efficiency reaches 91%. The reason why the efficiency is not so high because the transmission coils of the prototype are a scaled-down model. Thus,

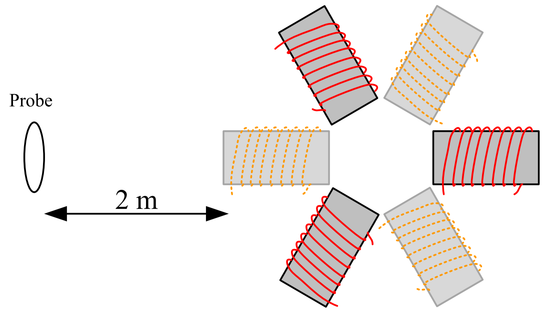

(a) For conventional three-phase IPT system

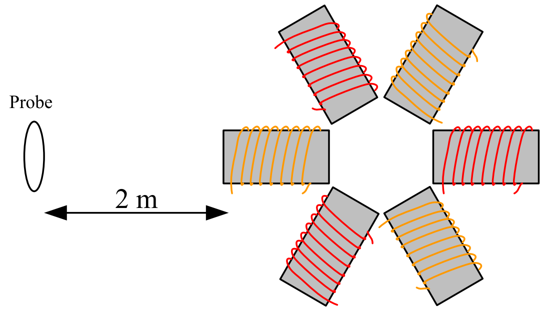

(b) For proposed three-phase IPT system

Fig. 8. Measurement of radiation noise

efficiency is expected to be improved in an actual application.

Figure 8 shows the measuring point of the radiation noise. The radiation noise is measured at 2 m from the coil edge. The radiation noise is measured in a shielded room. As the conventional system, the three-phase WPT system with three coils is tested for the comparison on the radiation noise. When the conventional method is tested, the six coils (coil B in Fig. 2) are removed. The transmission coils of phase-v and phase-w are placed in an angle of 120 degrees to the coils on phase-u.

Moreover, the radiation noise is compared under the same current condition because in principle the radiation noise from the loop coil is proportional to the current on the coils. By adjusting the current on the coils, the fair comparison can be achieved except the coil change. In order to remove the effect of the radiation noise from the inverter, the inverter is placed out of the shield room.

Figure 9 shows the radiation noise. Figure 9(a) is the radiation noise generated by the conventional three-phase WPT system with six coils where the coils B in Fig. 2 are removed. Figure 9(b) is the radiation noise generated by the proposed WPT system with 12 coils. The measurement distance and conditions are same as those in Fig. 9(a). In both the experiments, the common transmission coils are used. In order to have a fair comparison, the conduction currents on each coil are adjusted to be 6.0 A by adjusting the input DC voltage. The input DC voltage for the proposed 12 coils system is 393 V. On the other hand, the input DC voltage is reduced to 202 V for the conventional WPT system with six coils. Note that the inverter and the rectifier are put outside of the shielded room in order to evaluate only the radiation noise from the transmission coils.

The radiation noise at the fundamental frequency is suppressed from 12.2 dBμA to 2.1 dBμA by the proposed WPT system. It is confirmed that the proposed three-phase WPT

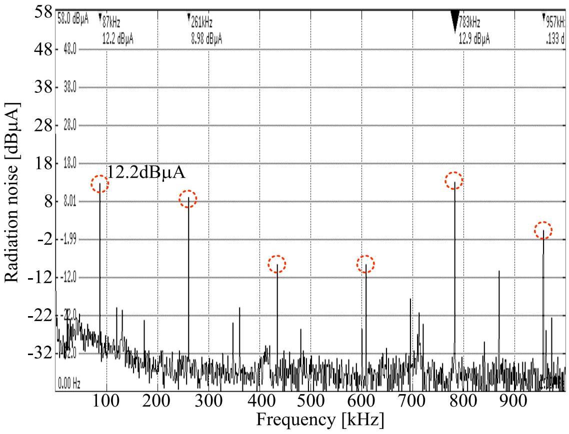

(a) Conventional three-phase IPT system with six coils

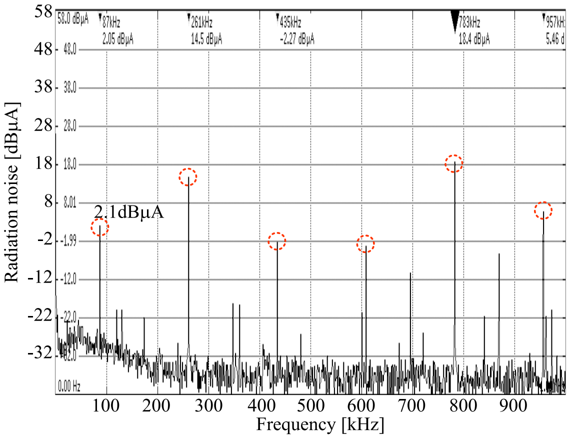

(b) Proposed three-phase IPT system with 12 coils

Fig. 9. Radiation noise at 2 m from the coil edge†

system is effective to reduce the fundamental radiation noise. However, the radiation noise on the third-order harmonics of the proposed system slightly increases.

5. Conclusion

This paper proposed three-phase wireless power transfer system. The proposed system has six primary coils and six secondary coils. The two coils on a phase are connected in series and these coils are differentially connected. The two coils reduce the radiation noise because the magnetic flux direction is opposite. Moreover, the six coils on each side allow to cancel out the magnetic interference among the multiple coils. Due to the cancel of the magnetic interference, the WPT system can be operated with an unity power factor of fundamental wave regarding the inverter output.

In this paper, the effect of the magnetic interference and its cancellation method is mathematically introduced. Then, the proposed scaled-mode was experimentally tested with the 3-kW prototype. The experimental results shows that the maximum DC-to-DC efficiency is 91%. Finally, the radiation noise is evaluated and compared to the conventional three-phase WPT system with six coils. The proposed method suppresses the radiation noise, which is measured at 2 m from the coil edge, from 12.2 dBμA to 2.1 dBμA on the fundamental frequency.

† It should be noted that the measurement method in this paper does not comply with the regulations published by CISPR.

References

(1) A. Kurs, R. Moffatt, and M. Soljacic: "Simultaneous mid-range power transfer to multiple devices", *Applied Physics Letters*, No.044102, pp.96–98 (2009)

(2) A. Kurs, A. Karalis, R. Moffatt, J.D. Joannopoulos, P. Fisher, and M. Soljacic: "Wireless Power Transfer via Strongly Coupled Magnetic Resonances", *Science*, Vol.317, pp.83–86 (2007)

(3) S. Weearsinghe, D.J. Thrimawithana, and U.K. Madawala: "Modeling Bidirectional Contactless Grid Interfaces With a Soft DC-Link", *IEEE Trans. On Power Electronics*, Vol.30, No.7, pp.3528–3541 (2015)

(4) F.Y. Lin, G.A. Covic, and J.T. Boys: "Evaluation of Magnetic Pad Sizes and Topologies for Electric Vehicle Charging", *IEEE Trans. On Power Electronics*, Vol.30, No.11, pp.6391–6407 (2015)

(5) M. Budhia, J.T. Boys, G.A. Covic, and C. Huang: "Development of a Single-Sided Flux Magnetic Coupler for Electric Vehicle IPT Charging Systems", *IEEE Trans. On Industrial Electronics*, Vol.60, No.1, pp.318–328 (2013)

(6) C. Huang, J.T. Boys, and G.A. Covic: "LCL pickup Circulating Current Controller for Inductive Power Transfer Systems", *IEEE Trans. On Power Electronics*, Vol.28, No.4, pp.2081–2093 (2013)

(7) T. Koyama, K. Umetani, and E. Hiraki: "Design Optimization Method for the Load Impedance to Maximize the Output Power in Dual Transmitting Resonator Wireless Power Transfer System", *IEEJ Journal of Industry Applications*, Vol.7, No.1, pp.49–55 (2018)

(8) T. Yamamoto, Y. Bu, T. Mizuno, Y. Yamaguchi, and T. Kano: "Loss Reduction of Transformer for LLC Resonant Converter Using a Magnetoplated Wire", IEEJ Journal of Industry Applications, Vol.7, No.1, pp.43–48 (2018)

(9) G. lovison, D. Kobayashi, M. Sato, T. Imura, and Y. Hori: "Secondary-side-only Control for High Efficiency and Desired Power with Two Converters in Wireless Power Transfer Systems", *IEEJ Journal of Industry Applications*, Vol.6, No.6, pp.473–481 (2017)

(10) K. Kusaka and J. Itoh: "Development Trends of Inductive Power Transfer Systems Utilizing Electromagnetic Induction with Focus on Transmission Frequency and Transmission Power", *IEEJ Journal of Industry Applications*, Vol.6, No.5, pp.328–339 (2017)

(11) R. Ota, N. Hoshi, and J. Haruna: "Design of Compensation Capacitor in S/P Topology of Inductive Power Transfer System with Buck or Boost Converter on Secondary Side", *IEEJ Journal of Industry Applications*, Vol.4, No.4, pp.476–485 (2015)

(12) International Organization for Standardization: "Electrically propelled road vehicles—Magnetic field wireless power transfer—Safety and interoperability requirements", Publicly available specification: ISO/PAS19363:2017(E)

(13) International Electrotechnical Commission: "Electric vehicle wireless power transfer (WPT) systems—Part 1: General requirements", International standard: IEC 61980-1 (2015)

(14) T. Shijo, K. Ogawa, M. Suzuki, Y. Kanekiyo, M. Ishida, and S. Obayashi: "EMI Reduction Technology in 85 kHz Band 44 kW Wireless Power Transfer System for Rapid Contactless Charging of Electric Bus", *IEEE Energy Conversion Congress & Expo 2016*, No.EC-0641 (2016)

(15) H. Narita, T. Imura, H. Fujimoto, and Y. Hori: "Electromagnetic Field Suppression in Polyphase Wireless Power Transfer", Technical report of IEICE, Vol.114, No.72, pp.39–44 (2014)

(16) M. Suzuki, K. Ogawa, F. Moritsuka, T. Shijo, H. Ishihara, Y. Kanekiyo, K. Ogura, S. Obayashi, and M. Ishida: "Design method for low radiated emission of 85 kHz band 44 kW rapid charger for electric bus", *IEEE Applied Power Electronics Conference and Exposition 2017*, pp.3695–3701 (2017)

(17) T. Shijo, K. Ogawa, F. Moritsuka, M. Suzuki, H. Ishihara, Y. Kanekiyo, K. Ogura, M. Ishida, S. Obayashi, S. Shimmyo, K. Maki, F. Takeuchi, and N. Tada: "85 kHz band 44 kW wireless power transfer system for rapid contactless charging of electric bus", *International Symposium on Antennas and Propagation 2016*, pp.38–39 (2016)

(18) D.J. Thrimawithana, U.K. Madawala, A. Francis, and M. Neath: "Magnetic Modeling of a High-Power Three Phase Bi-Directional IPT System", *37th Annual Conference of the IEEE Industrial Electronics Society*, pp.1414–1419 (2011)

(19) G.A. Covic, J.T. Boys, M.L.G. Kissin, and H.G. Lu: "A Three-Phase Inductive Power Transfer System for Roadway-Powered Vehicles", *IEEE Trans. on Industrial Electronics*, Vol.54, No.6, pp.3370–3378 (2007)

(20) A. Laka, J.A. Barrena, J. Chivite-Zabalza, M.A. Rodriguez, and P. Izurza-Moreno: "Isolated Double-Twin VSC Topology Using Three-Phase IPTs for High-Power Applications", *IEEE Trans. on Power Electronics*, Vol.29, No.11, pp.5761–5769 (2014)

(21) M. Kim, S. Ahn, and H. Kim: "Magnetic Design of a Three-Phase Wireless Power Transfer System for EMF Reduction", *IEEE Conference on Wireless Power Transfer Conference 2014*, pp.17–20 (2014)

(22) Y.H. Sohn, B.H. Choi, E.S. Lee, G.C. Lim, G. Cho, and C.T. Rim: "General Unified Analyses of Two-Capacitor Inductive Power Transfer Systems: Equivalence of Current-Source SS and SP Compensations", *IEEE Trans. On Power Electronics*, Vol.30, No.11, pp.6030–6045 (2015)

(23) International Special Committee on Radio Interference: "Industrial, scientific and medical equipment—Radio-frequency disturbance characteristics—Limits and methods of measurement", CISPR 11: 2015 (2015)

(24) R. Steigerwald: "A comparison of half-bridge resonant converter topologies", IEEE Trans. on Power Electronics, Vol.3, No.2, pp.174–182 (1988)

(25) R. Bosshard, J.W. Kolar, J. Muhlethaler, I. Stevanovic, B. Wunsch, and F. Canales: "Modeling and eta-alpha-Pareto Optimization of Inductive Power Transfer Coils for Electric Vehicles", IEEE Journal of Emerging and Selected Topics in Power Electronics, Vol.3, No.1, pp.50–64 (2015)

Keisuke Kusaka (Member) received his B.S. and M.S. degrees from Nagaoka University of Technology, Niigata, Japan in 2011, 2013, respectively. From 2015 to 2016, he was with Swiss Federal Institute of Technology in Lausanne (EPFL), Switzerland as a trainee. In 2016, he received his Ph.D. degree in energy and environment science from Nagaoka University of Technology. From 2016 to 2018, he was with Nagaoka University of Technology as a researcher. He is currently an assistant professor at Nagaoka University of Technology. His current research interests include an inductive power transfer system and high-frequency converters. He received the second prize paper award in IPEC-Niigata 2018.

Keita Furukawa (Student Member) received his B.S. and M.S. degrees in electrical, electronics and information engineering from Nagaoka University of Technology, Niigata, Japan in 2016 and 2018, respectively. He is currently a Ph.D. candidate at Nagaoka University of Technology, Niigata, Japan. His research interests include an inductive power transfer. He is a member of the Institute of Electrical Engineers of Japan and the Institute of Electrical and Electronics Engineers.

Jun-ichi Itoh (Senior Member) was born in Tokyo, Japan, in 1972. He received his M.S. and Ph.D. degree in electrical and electronic systems engineering from Nagaoka University of Technology, Niigata, Japan in 1996, 2000, respectively. From 1996 to 2004, he was with Fuji Electric Corporate Research and Development Ltd., Tokyo, Japan. He was with Nagaoka University of Technology, Niigata, Japan as an associate professor. Since 2017, he has been a professor. His research interests are matrix converters, dc/dc converters, power factor correction techniques, energy storage system and adjustable speed drive systems. He received IEEJ Academic Promotion Award (IEEJ Technical Development Award) in 2007. In addition, he also received Isao Takahashi Power Electronics Award in IPEC-Sapporo 2010 from IEEJ, 58th OHM Technology Award from The Foundation for Electrical Science and Engineering, November, 2011, Intelligent Cosmos Award from Intelligent Cosmos Foundation for the Promotion of Science, May, 2012, and Third prize award from Energy Conversion Congress and Exposition-Asia, June, 2013. Prizes for Science and Technology (Development Category) from the Commendation for Science and Technology by the Minister of Education, Culture, Sports, Science and Technology, April 2017. Dr. Itoh is a senior member of the Institute of Electrical Engineers of Japan, the Society of Automotive Engineers of Japan and the IEEE.